International Journal of Geo-Information

MDPI

Article

Impact of Land Use Change on Carbon Storage in Complex Terrains: A Case Study of Sichuan–Chongqing, China

Tiankuo Chu [1,2], Jun Li [1,*], Chengye Zhang [1], Xiaoai Dai [2], Yikun Qing [3], Huan Huang [4,5] and Manling Peng [1]

[1] College of Geoscience and Surveying Engineering, China University of Mining and Technology, Beijing 100083, China; tiankuochu@student.cumtb.edu.cn (T.C.); czhang@cumtb.edu.cn (C.Z.); pml@student.cumtb.edu.cn (M.P.)
[2] College of Geography and Planning, Chengdu University of Technology, Chengdu 610059, China; daixiaoa@cdut.edu.cn
[3] College of Social Science, Duke Kunshan University, Kunshan 215300, China; yq92@duke.edu
[4] College of Business, Chengdu University of Technology, Chengdu 610059, China; huan@cdut.edu.cn
[5] Digital Hu Huanyong Line Research Institute, Chengdu University of Technology, Chengdu 610059, China
* Correspondence: junli@cumtb.edu.cn

Abstract: Understanding human activity and global climate change requires an understanding of the impact of land-use change on carbon storage. Nevertheless, the number of studies examining carbon storage in complex terrain areas remains relatively limited. This study quantified land use shifts and carbon storage variations from 2010 to 2030 in the Sichuan–Chongqing region in China by combining InVEST and PLUS models. The results show that (1) the Sichuan–Chongqing region exhibits a predominantly concentrated pattern of land utilization, with forests occupying a dominant position among various land types in the locality. (2) The total carbon storage loss between 2010 and 2020 is 24.19 Tg. Except for the ecological development scenario, compared to 2020, all multi-scenario projections show less carbon storage in 2030. (3) The primary cause of carbon loss is the sprawl of built-up areas into farmlands, forests, and grasslands. (4) The geomorphology of complex terrain greatly affects carbon storage; flat terrain tends to be less carbon-intensive than more steeply sloping terrain. This study offers worthwhile insights for sustainable land management and carbon mitigation strategies in complex terrains worldwide.

Keywords: land-use change; carbon storage; complex terrain; multiscenario simulation; Sichuan–Chongqing region

check for updates

Citation: Chu, T.; Li, J.; Zhang, C.; Dai, X.; Qing, Y.; Huang, H.; Peng, M. Impact of Land Use Change on Carbon Storage in Complex Terrains: A Case Study of Sichuan–Chongqing, China. *ISPRS Int. J. Geo-Inf.* **2024**, *13*, 428. https://doi.org/10.3390/ijgi13120428

Academic Editors: Wolfgang Kainz, Jingzhe Wang, Yangyi Wu, Yinghui Zhang, Ivan Lizaga and Zipeng Zhang

Received: 8 October 2024
Revised: 22 November 2024
Accepted: 27 November 2024
Published: 29 November 2024

Copyright: © 2024 by the authors. Published by MDPI on behalf of the International Society for Photogrammetry and Remote Sensing. Licensee MDPI, Basel, Switzerland. This article is an open access article distributed under the terms and conditions of the Creative Commons Attribution (CC BY) license (https://creativecommons.org/licenses/by/4.0/).

1. Introduction

Carbon storage in terrestrial ecosystems is influenced both by non-anthropogenic factors, like climate and atmospheric composition, and human activities, for example, land cover and management measures [1]. Understanding and monitoring carbon storage on terrestrial ecosystems could prove crucial in elucidating the linkages among carbon storage, climate change, and biodiversity for sustainable development [2,3]. Land use change is the second-most influential factor in terms of its impact on increasing atmospheric carbon dioxide concentrations, and the variations in carbon storage within terrestrial ecosystems correlate strongly with land use change [4].

Significant variations in carbon sequestration capacities are observed across different land use [5], and grassland contains more carbon storage than land does, such as construction land and farmland. Land use dynamics significantly affect the overall carbon stock of regional terrestrial ecosystems [6]. Therefore, assessing ecosystem carbon storage under current land use and modelling changes in it subject to future changes in land use are conducive to the efficient and rational use the limited natural resources. This is highly important for achieving sustainable development and carbon neutrality.

In recent years, studies on regional carbon storage estimation can be split into two categories. The first category is grounded in measurements at sample sites, with the results extended to the regional scale via various methods, such as calculating the change in regional carbon storage using the biomass conversion method [7,8] or analysing the exchange relationship between terrestrial ecosystems and atmospheric carbon dioxide to estimate carbon storage from the viewpoint of micrometeorology [9]. However, conventional carbon storage estimation methodologies are time-consuming, labour-intensive, constrained by observational outcomes, and prone to data gaps [10]. Moreover, these approaches do not adequately consider spatial coherence of terrestrial ecosystems, and there is uncertainty and error in the transformation process from the sampling point to the whole study area, which makes it impossible to calculate regional carbon stocks for a larger area [11]. The second category involves estimating regional carbon storage using geographic information science (GIS) and remote sensing models. An illustrative example is the Geographically Weighted Regression (GWR) model [12], which can be integrated with sample data and other remotely sensed metrics to model the spatial heterogeneity of ecosystem carbon density. Furthermore, the Terrestrial Ecosystem Dynamic Model (TEM) [13] and the Ecological Process Model (Biome-BGC) [14] are also widely employed, these models elucidate the carbon cycling patterns of ecosystems by calculating the relevant physiological and ecological parameters for different ecosystem types. Another notable model is the CASA model [15], which estimates carbon storage based on factors such as effective solar radiation, temperature, and water availability. Moreover, researchers have increasingly combined deep learning techniques [16] with other remote sensing models to estimate carbon storage [17]. While these models contribute to a comprehensive understanding of the dynamics of regional carbon stocks, they often overlook certain environmental and ecological factors, may lack accuracy, and generally lack the flexibility for adjustments and refinements based on specific conditions. The Integrated Valuation of Ecosystem Services and Tradeoffs (InVEST) model is commonly used to assess and estimate the carbon storage and sequestration capacity of ecosystems. Compared to other traditional estimation models, this module is mainly based on the carbon pools of forest ecosystems but also takes into account other ecosystems like grass-lands, wetlands and farmlands [18]. The model requires less data and is easier to obtain, so it achieves good results in calculating carbon storage [19–21].

Given the accelerated rate of urbanisation and global warming, it is crucial to allocate land resources correctly, maintain land use patterns, and ensure a stable level of carbon storage [22]. A single carbon storage estimation model can only determine the total amount of carbon storage in the current region, but it is unable to predict and estimate the dynamic pattern of regional carbon storage changes in future time scales, nor can the drivers of regional carbon storage changes be explored through modelling approaches. To tackle this challenge, researchers are assessing regional carbon storage while considering the multidimensional socioeconomic and ecological benefits. They have estimated future carbon storage in regional terrestrial ecosystems and the factors driving carbon storage changes by combining traditional carbon storage estimation models with land type dynamics prediction models. In these land use type prediction models, the Conversion of Land Use and its Effects at Small Regional Extent (CLUE-S) model evaluates the suitability of regional unused land and simulates the optimisation of land use in accordance with the local ecological environment [23]. Moreover, the Future Land Use Simulation (FLUS) model combines system dynamics and meta-cellular automata models to simulate multiple scenarios considering various socioeconomic and natural climate factors [24]. However, the Patch-Generating Land Use Simulation (PLUS) model has benefits in predicting the status of carbon storage under future development scenarios. It is more effective than models such as FLUS at determining the drivers behind land expansion and predicting the distribution of land-use landscapes at the pixel scale [25].

Combining the strengths of the InVEST model and the PLUS model can address the limitations of a single model for carbon storage estimation and deepen the understanding of the dynamic relationship between land use change and carbon storage, this research

examined patterns in land use and regional carbon storage changes over time and space in a complex terrain region, with the Sichuan–Chongqing area being the focal point. Multiple scenarios of 2030 land use were performed using the PLUS model, while changes in drivers were simultaneously analysed and subsequently, integrated with the InVEST model, we delved into the space–time-evolving patterns of carbon storage and intended to delve into the following key inquiries: (1) What are the distinctions in land use between the Sichuan–Chongqing region over the past decade? (2) What are the spatial and temporal patterns for carbon stocks estimated from the land use distribution results from multiple scenario simulations in this region? (3) What are the main drivers of land change carbon change in Sichuan–Chongqing? The findings of this study will aid in the optimisation of land use structure in complex terrain regions such as the Sichuan–Chongqing region. This approach will facilitate the rationalization of spatial resource planning, sustain carbon sequestration at optimal levels, and expedite the achievement of carbon neutrality.

2. Materials and Methods

2.1. Study Area

The Sichuan–Chongqing area is situated in the southwest of China. It comprises the province of Sichuan and the municipality of Chongqing (Figure 1). The region spans approximately 568,000 square kilometres and features a complex topography, including mountainous, plateau, and basin landscapes, as well as abundant natural resources. The climate is typical of a subtropical monsoon, with high temperatures and precipitation during the summer. The study areas of Sichuan and Chongqing are experiencing rapid economic development, with the city cluster centred around Chongqing becoming a strategic hub for China. The local government has ordered the full implementation of the new development concept and promote the early formation of a carbon peak and a carbon-neutral pattern.

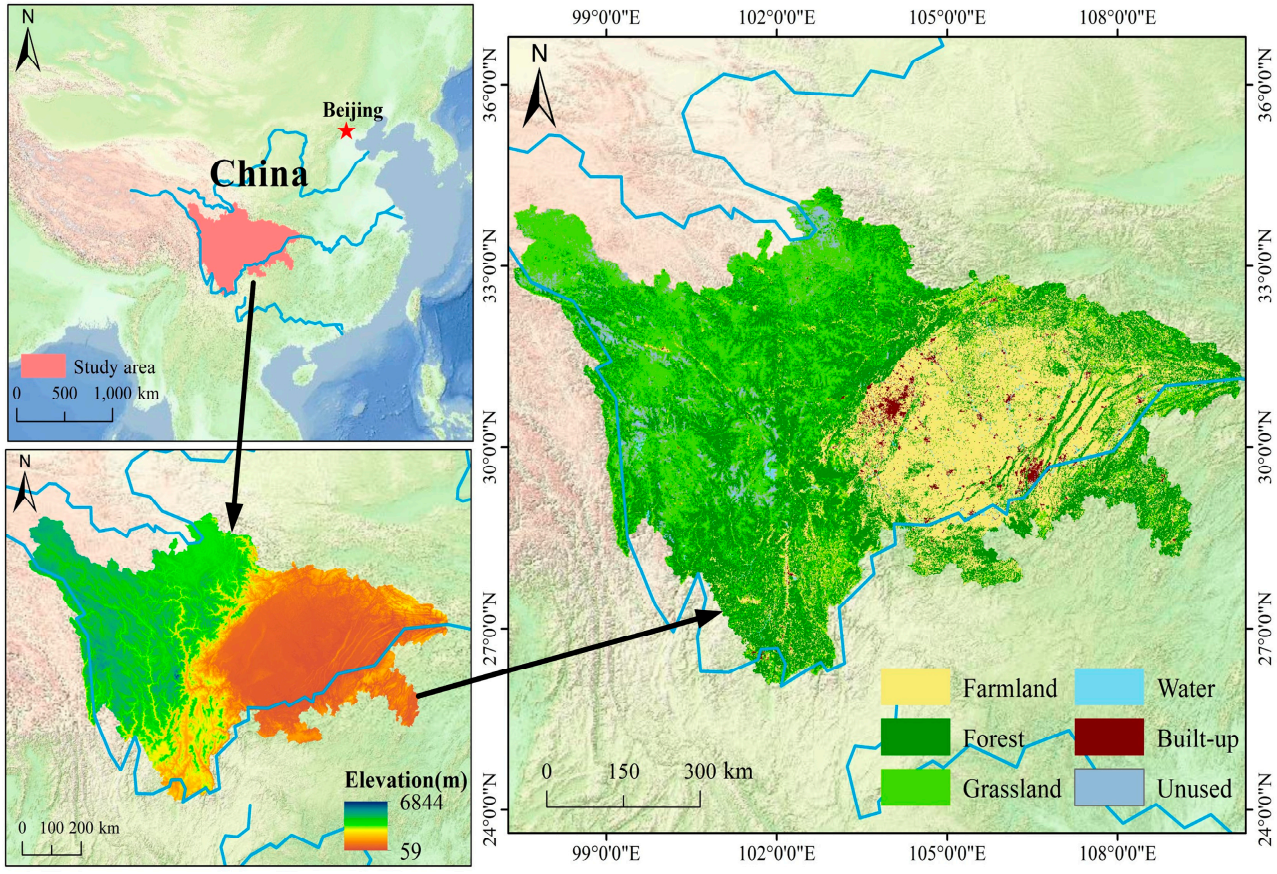


Figure 1. Location of Sichuan–Chongqing region in China.

2.2. Data Resources

In order to investigate the spatial and temporal patterns and drivers of carbon storage under land use change, this study collected multi-source datasets, as shown in Table 1. These datasets include land use data for carbon storage estimation and prediction, as well as natural factors (DEM, slope, rainfall, etc.) and anthropogenic factors (GDP, population, etc.) for the purpose of analysing the drivers of carbon storage change. The land use data was classified into six categories: farmland, grassland, forest, water, built-up, and unused. Additionally, the study used population and GDP data from 2019 because 2020 data were unavailable. The city-level road data and motorways were processed via the ArcGIS Euclidean distance function. All the data were uniformly adjusted to a 1-kilometre resolution via the resampling method.

Table 1. List of data base and its sources used for this study.

Data	Year	Resolution	Data Resource
Land use	2010–2020	1000 m	https://www.resdc.cn/ (accessed on 5 May 2024)
Land use constraints	2020	1000 m	Obtained through processing of land use data (accessed on 5 May 2024)
Soil type	1995	1000 m	https://www.resdc.cn/ (accessed on 5 May 2024)
Average annual temperature	2020	1000 m	https://www.resdc.cn/ (accessed on 5 May 2024)
Average annual precipitation	2020	500 m	https://cds.climate.copernicus.eu/ (accessed on 5 May 2024)
DEM	2020	90 m	http://www.gscloud.cn/home (accessed on 5 May 2024)
Slope	2020	90 m	Obtained through processing of DEM data
GDP	2019	1000 m	https://www.resdc.cn/ (accessed on 5 May 2024)
Population	2019	1000 m	https://www.resdc.cn/ (accessed on 5 May 2024)
Urban primary roads	2020	Vector data	https://www.openhistoricalmap.org/ (accessed on 5 April 2024)
Urban secondary roads	2020	Vector data	https://www.openhistoricalmap.org/ (accessed on 5 April 2024)
Urban tertiary roads	2020	Vector data	https://www.openhistoricalmap.org/ (accessed on 29 April 2024)
Highways	2020	Vector data	https://www.openhistoricalmap.org/ (accessed on 29 April 2024)
Rivers	2020	Vector data	Obtained through processing of DEM data
Government locations	2020	Vector data	https://www.webmap.cn/ (accessed on 5 May 2024)

2.3. Methods

This study aimed to examine the spatial and temporal variations of land use and carbon storage in complex terrain areas. To achieve this, land use data, carbon intensity data and related driver information were used in conjunction with the InVEST and PLUS models. Furthermore, a multi-scenario emulation on land use in the Sichuan–Chongqing region was conducted along with an investigation into the driving factors and distributional differences of carbon density in complex terrain areas. Depicted in Figure 2 is the study's flowchart.

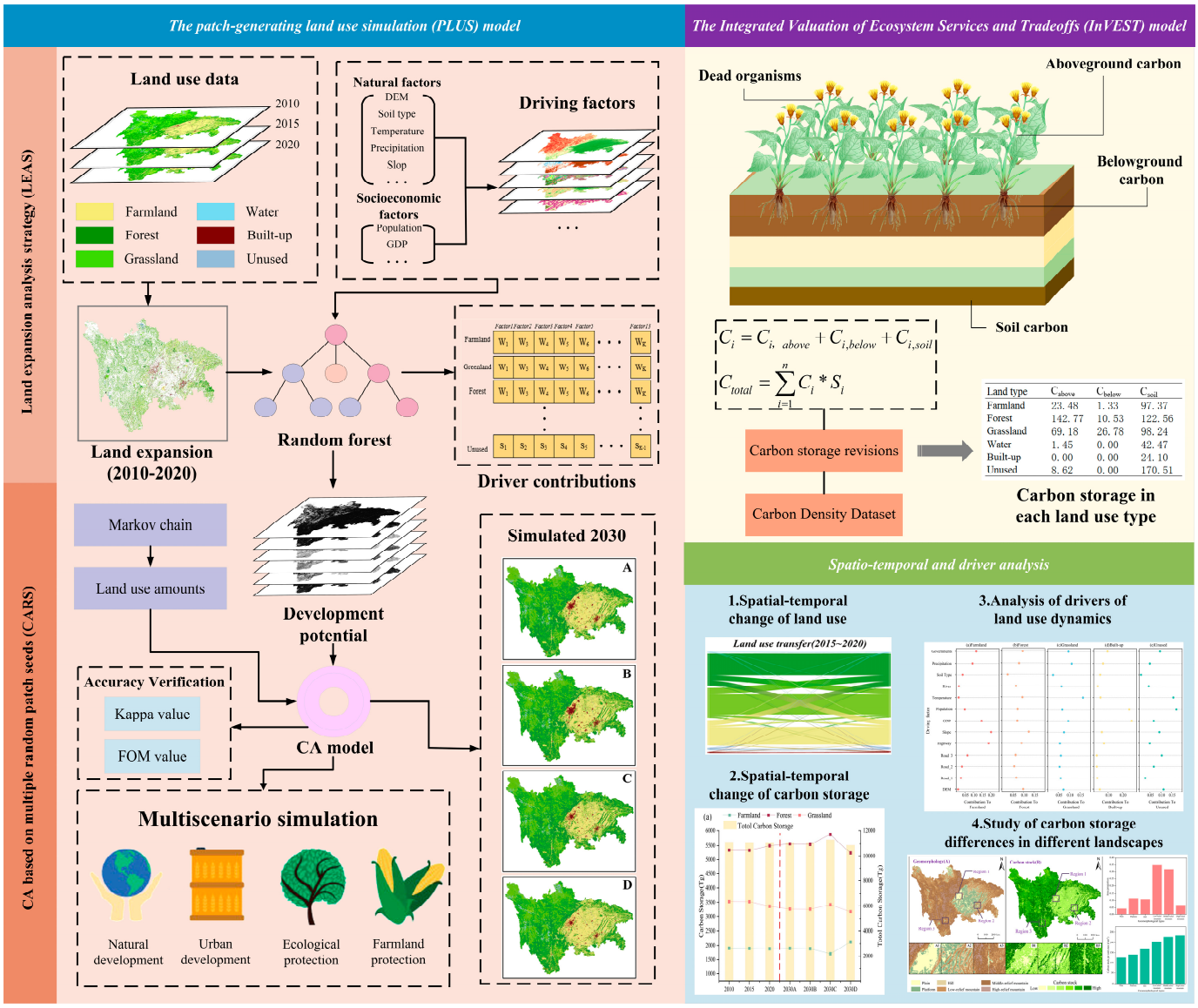


Figure 2. Flowchart.

2.3.1. Carbon Storage Estimation Modelling and Correction

To estimate regional carbon storage, the carbon assessment feature of the InVEST framework was utilized, which distinguishes carbon stock in terrestrial ecosystems into four elements: (1) carbon storage in aboveground biomass, (2) carbon storage in belowground biomass, (3) carbon storage in organic carbon in soils, and (4) carbon storage in dead organisms [26]. The model excludes highly unstable carbon that can easily oxidise, decompose and be released into the atmosphere. In addition, only three carbon components were considered in this study because of limitations in data acquisition for the fourth component [27].

$$C_t = C_{t,above} + C_{t,below} + C_{t,soil} \quad (1)$$

$$C_{sum} = \sum_{t=1}^{n} C_t * S_t \quad (2)$$

where C_t stands for the carbon density for land-use type t; the variables $C_{t,above}$, $C_{t,below}$, and $C_{t,soil}$ represent the three components contributing to carbon density within this land use classification: carbon in aboveground biomass, carbon in belowground biomass, and soil organic carbon at a depth of 0–100 cm; and C_{sum} is the sum carbon storage in this region.

S_t refers to area of tth type; variable n denotes quantity of defined land types in the study area, which is set to 6 for this analysis.

The above-ground biomass carbon storage and 0–100 cm soil carbon storage data were acquired from the 2010 China Terrestrial Ecosystem Carbon Density Dataset [28]. For the below-ground biomass component, the carbon storage was calculated using the biomass factor conversion method as follows:

$$C_{t,below} = a * b * W_{D,t} \tag{3}$$

where $W_{D,t}$ is above-ground biomass for land type t; a is the transformation factor; b is the proportion of below-ground to above-ground biomass; and above-ground biomass refers to the relevant research results [29,30], with a values of 5 and b values of 0.19, 0.25, and 5.2 for farmland, forest, and grassland, respectively.

In terms of the sources of carbon for these two components of aboveground biomass and soil, due to data limitations, it is difficult to directly obtain the relevant carbon storage parameters in our study region. To increase the reliability of carbon stock calculations, this paper uses a connection model between carbon density and precipitation to calibrate the results [31]. The relation model is as follows: (The final result calculated by InVEST carbon model is shown in Table A1).

$$C_{BP} = 6.789 * e^{0.0054 * P_{MA}} \tag{4}$$

$$C_{SP} = 3.3968 * P_{MA} + 3996.1 \tag{5}$$

$$K_{BP} = C_{BP1} / C_{BP2} \tag{6}$$

$$K_{SP} = C_{SP1} / C_{SP2} \tag{7}$$

where C_{BP} is the carbon density determined from annual precipitation, P_{MA} is the annual precipitation, K_{BP} is the calibration factor for the precipitation coefficient of aboveground biomass carbon density, K_{SP} is the calibration factor for the precipitation coefficient of soil carbon density, and C_{BP1} and C_{BP2} are the aboveground carbon density correction coefficients, which are taken from the mean annual precipitation of Sichuan–Chongqing region and the nationwide average annual precipitation separately in Formula (4). C_{SP1} and C_{SP2} are brought into Formula (5) according to the average annual precipitation of the Sichuan–Chongqing region as well as the national average annual precipitation.

2.3.2. Land Expansion Analysis Strategy (LEAS) Modelling

LEAS module of the PLUS model assesses the feasibility and suitability of land use by analysing the current status and trends of land use in a city or region. The model uses a random forest algorithm to examine land use expansion and its drivers on a case-by-case basis. It calculates the probability of development for different sites and assesses the contribution of each driver to land expansion over a specified time period, which is calculated using the formula shown below [25]:

$$P^d_{i,k(X)} = \sum_{n=1}^{M} I[h_n(X) = d] / M \tag{8}$$

where X represents a vector of various driving factors and M represents the decision tree number employed. d is a binary variable that takes values of 0 and 1, where 0 means that land type k does not allow the transfer of other land and 1 indicates that they can be transformed; $h_n(X)$ is its forecasted land type obtained by evaluating the decision tree n in the set. $I[h_n(X) = d]$ is a function that represents the probability that a land type k undergoes expansion in image i conditioned on the value of d and given the input X.

2.3.3. CA Based on Multiple Random Patch Seeds (CARS) Modelling

The CARS modelling within the PLUS framework, building upon the traditional binary state space, introduces multiple "types" or "species" that can interact with each other, enabling the simulation of intricate phenomena. This model is capable of simulating future land use across vast regions. In this study, the CARS model was employed to calculate the spatial distribution and development of future carbon storage by obtaining the development probability of different land to emulate and predict future land change. The total conversion probability $P_{O,i,k}^{d=1,t}$ of land type k is given by [25]:

$$P_{O,i,k}^{d=1,t} = P_{i,k}^{d=1} * \Omega_{i,k}^{t} * D_{k}^{t} \tag{9}$$

$$\Omega_{i,k}^{t} = \frac{\mathrm{con}(c_{i}^{t-1} = k)}{n * n - 1} * w_{k} \tag{10}$$

$$D_{k}^{t} = \begin{cases} D_{k}^{t-1} & \left(\left|G_{k}^{t-1}\right| \leq \left|G_{k}^{t-2}\right|\right) \\ D_{k}^{t-1} * \frac{G_{k}^{t-2}}{G_{k}^{t-1}} & \left(G_{k}^{t-1} < G_{k}^{t-2} < 0\right) \\ D_{k}^{t-1} * \frac{G_{k}^{t-1}}{G_{k}^{t-2}} & \left(0 < G_{k}^{t-2} < G_{k}^{t-1}\right) \end{cases} \tag{11}$$

where $P_{O,i,k}^{d=1,t}$ is the likelihood that pixel i will be a land of class k in the future; $\Omega_{i,k}^{t}$ is the perturbation of this pixel to the surrounding neighbourhood; and D_{k}^{t} represents the level of demand for land k. In Equations (10) and (11), con is the number of pixels of kth class in the $n * n$ window of the results of the final iteration; w_k is the value of the weights among the land types, defaulting to 1; and G_{k}^{t-1} and G_{k}^{t-2} are the variance in requirements for land type k between the present demand at iteration $t-1$ and the future demand at iteration $t-2$.

2.3.4. Setting of Land Development Scenarios

In order to clarify the differences in land use patterns and carbon storage under different development plans in topographically complex regions, and to capture the spatial and temporal variation patterns of carbon storage, this study sets up four different development scenarios applicable to the Sichuan–Chongqing region, taking into account the current development status and policies of the study region, as well as the land use conditions, and referring to the existing multi-scenario land use simulation framework [32,33]. The scenario setting process takes into account the differences in development policies and the rationality of scenario setting, and determines the differences in land use transfer under different scenarios [34]:

(1) Natural development scenario: Without any other modifications to the land use transfer matrix, the previous land transfer probabilities continued, but owing to the relative stability of water, the transfer of water is constrained in the forecasting process of this study.

(2) Urban development scenario: In this context, economic development is identified as the overarching objective, especially the development of built-up land. In the forecast analysis, the likelihood of conversion of built-up land to alternative land types decreases by 20 percent, while the likelihood of other land being converted to built-up areas increases by 20 percent.

(3) Ecological protection scenario: Green development is set as the primary objective in this scenario, with a 20 percent reduction in the odds of converting forests and grasslands to different types. The probability of converting land types other than building land to forest and grassland increases by 20 percent.

(4) Farmland protection scenario: The probability of transferring farmland to other land types decreases by 20 percent, whereas the probability of transferring other land types to farmland increases by 20 percent under this scenario, compared to the transfer probability under the natural development scenario.

3. Results

3.1. Spatial–Temporal Change of Land Use in the Sichuan–Chongqing Region from 2010 to 2020

3.1.1. Land Use Distribution in the Sichuan–Chongqing Region from 2010 to 2020

The spatial distribution of land use patterns in Sichuan–Chongqing region was relatively concentrated (Table 2, Figure 3). Forests, encompassing woodlands, open forests, and scrublands, dominated the region, occupying between 34.59% to 35.20% of the total area. They were primarily distributed in the western Sichuan plateau region, one of the most topographically complex regions in China, located somewhere in the middle of the Qinghai–Tibet plateau and the Sichuan Basin. Grassland, farmland, and unused land accounted for 30.63% to 32.52%, 27.27% to 27.89%, and 3.07% to 3.27% of the total area, respectively. Water and built-up land occupy a smaller proportion of the whole region, accounting for 0.86% to 1.04% and 0.83% to 1.52%, respectively. The majority of built-up was concentrated in Chengdu and its adjacent regions, as well as within the Chongqing Metropolitan Area and the Sichuan–Chongqing economic region. Notably, the proportion of farmland in this region surpassed the national average of 14.3%, whereas the proportion of built-up land remained below the national average of 4%.

Table 2. Distribution of land types by year in Sichuan and Chongqing (km^2).

Land Type	2010		2015		2020	
	Area	Proportion	Area	Proportion	Area	Proportion
Farmland	155,858	27.89%	155,236	27.78%	154,376	27.27%
Forest	193,484	34.62%	193,263	34.59%	199,213	35.20%
Grassland	181,707	32.52%	181,516	32.48%	173,366	30.63%
Water	4831	0.86%	5137	0.92%	5892	1.04%
Built-up	4661	0.83%	6348	1.14%	8604	1.52%
Unused	18,262	3.27%	17,303	3.10%	17,352	3.07%

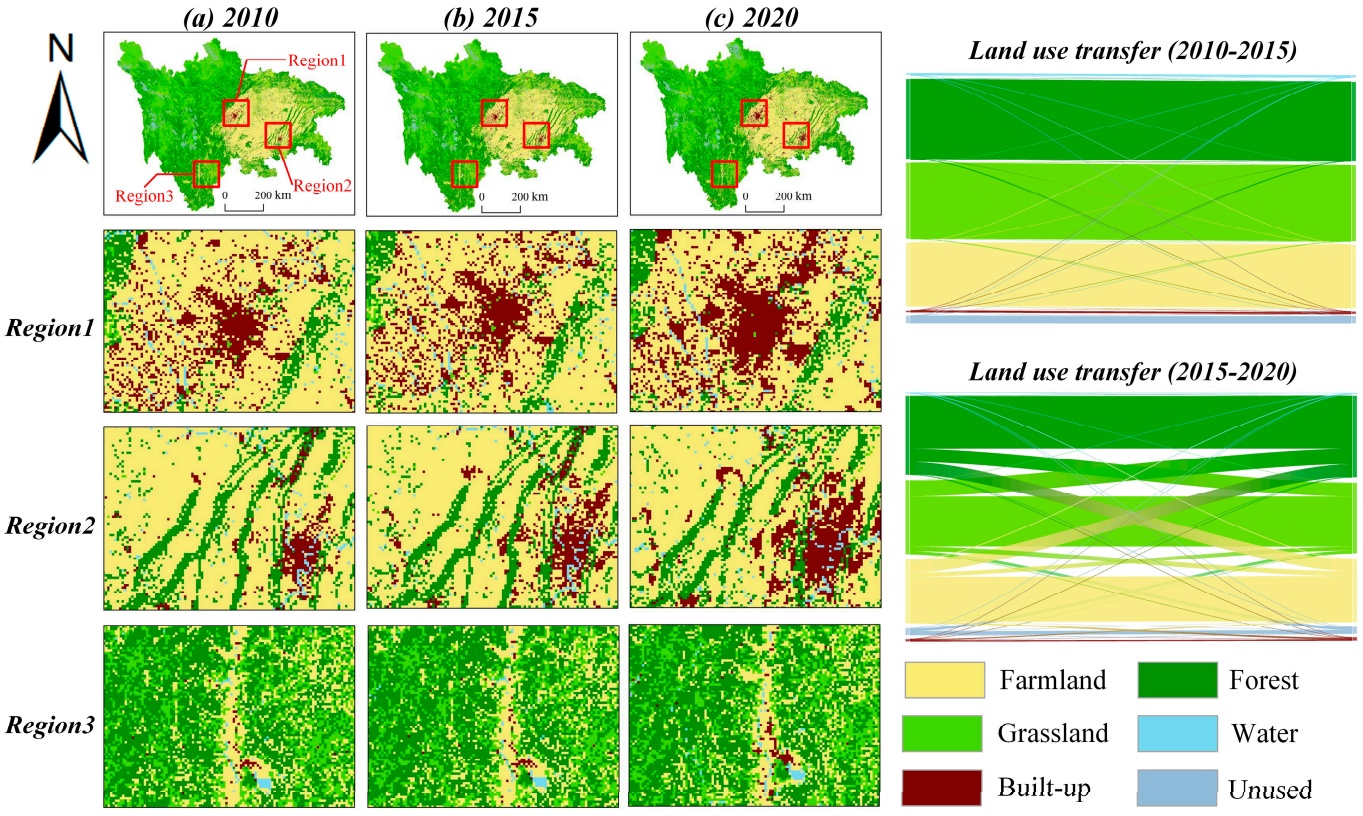


Figure 3. Land use distribution and land transfer in the Sichuan–Chongqing area.

From a temporal perspective, area changes between 2010 and 2020 varies considerably among land types, with the most notable change occurring in built-up, which increased from 0.83% to 1.52%, almost doubling in just a decade, expanding by 3943 km^2. Additionally, the area of forests (+5729 km^2, +0.58%) and watersheds (+1061 km^2, +0.18%) also showed increasing trends. In contrast, the other three land types in the region exhibited a downward trend during this period. In terms of area change, grassland decreased the most (−8341 km^2, −1.89%), followed by farmland (−1482 km^2, −0.62%) and unused land (−910 km^2, −0.20%).

3.1.2. Land Use Transfer in the Sichuan–Chongqing Region from 2010 to 2020

To gain insight into the diversity of land use changes in the Sichuan–Chongqing region, as well as the specific direction of flow, a land use transfer study was conducted using a land use matrix (Table A2). The findings indicated that a total of 5,879,400 hm^2 of grassland was converted from 2010 to 2020. The majority of these conversions were into forest, accounting for 3,852,300 hm^2 or 65.52% of the total converted area. In addition, approximately 19.58% of the grassland area transferred to farmland, and approximately 1.63% was converted into built-up land. A total of 4,665,700 hm^2 of farmland was transferred out, of which forest was the largest source of transfer, with an area of 2,985,100 hm^2, accounting for 63.98%. Another 20.55% of the area was converted to grassland, with an area of 958,700 hm^2. A total of 646,600 hm^2 of built-up land was transferred, with 491,700 hm^2 (76.04%) sourced from farmland, marking it as a primary reason for the enlargement of built-up land over the past decade. Moreover, a discernible interplay existed between farmland, built-up land, and water, with 22.59 hm^2 of farmland transformed to water, while 18.81 hm^2 of water was converted back to farmland. Additionally, 49.17 hm^2 of farmland was converted to built-up land, and 18.08 hm^2 of built-up land was returned to farmland.

3.2. Multi-Scenario Simulation of Spatial and Temporal Carbon Storage Changes in the Sichuan–Chongqing Region from 2010 in 2030

3.2.1. Spatiotemporal Changes in Land Use in the Sichuan–Chongqing Region Under Multiple Scenarios

Taking the land use status of Sichuan–Chongqing region in 2020 as the initial state of simulation, we applied the CARS model combined with the Markov chain model to derive land use distribution situation of each scenario in 2030 (Table 3, Figure 4). The CARS model parameters are shown in Table A3. In this study, the 2010 land use data was employed to simulate and validate the 2020 land use data, resulting in a kappa coefficient of 0.892 and an FOM value of 0.191. These findings substantiate the feasibility of multi-scenario simulation in this study area. The research findings show that the spatial distribution pattern of land use will not undergo significant changes by 2030 under various development scenarios. In terms of development scenarios, the expansion directions of built-up in all four development scenarios are essentially the same, extending outwards from the areas in 2020, albeit at varying speeds. The urban development scenario has the fastest expansion rate, while the farmland protection scenario has the slowest expansion rate. In terms of regional development, the original urban clusters of Chengdu and Chongqing are undergoing the fastest expansion. Furthermore, regions such as Yibin, Luzhou, and Nanchong are developing increasingly prominent construction land clusters, especially under the urban development scenario. Changes in forest and grassland are primarily concentrated around the Sichuan Basin, expanding towards the centre of the basin, with particularly evident ecological protection scenarios. The protection of farmland slows down the expansion rate of forest and grassland towards the centre in the farmland protection scenario.

Table 3. The area of each land use (km^2) (A, B, C, and D represent the scenarios of natural development, urban development, ecological protection, and farmland protection).

Land Type	Scenario			
	A	B	C	D
Farmland	155,608	154,570	139,813	174,016
Forest	201,578	200,852	212,630	189,953
Grassland	168,498	168,298	176,160	163,638
Water	5892	5892	5892	5892
Built-up	10,444	12,588	9854	8882
Unused	16,783	16,603	14,454	16,422

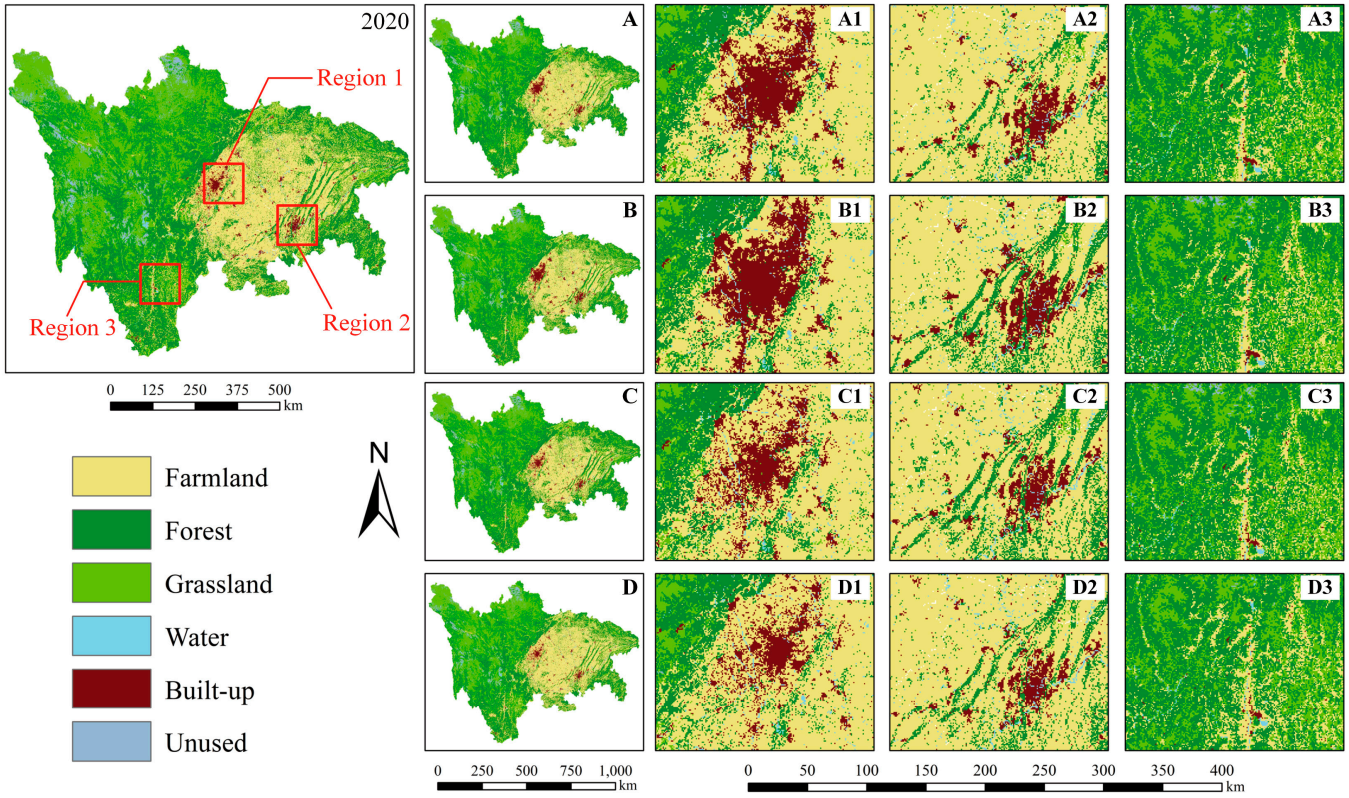


Figure 4. Land use under each scenario (**A**–**D** represent the scenarios of natural development, urban development, ecological protection, and farmland protection in the Sichuan–Chongqing region in 2030, respectively. Regions 1, 2, and 3 are enlarged example regions).

3.2.2. Estimation and Prediction of the Spatial and Temporal Evolution of Carbon Storage in Sichuan–Chongqing Region

The InVEST model was employed to quantify carbon storage for individual land type as well as the entire Sichuan–Chongqing region's total carbon storage from 2010 to 2030 (Table 4, Figure 5). The findings showed that the total carbon storage decreased from 11,130.07 Tg to 11,105.88 Tg between 2010 and 2020, resulting in a decrease of 24.19 Tg in total carbon storage. It also shows a downward trend from 2020 to 2030 across various development scenarios, with the exception of the eco-development scenario. The total carbon stock in the natural development scenario is projected to be reduced by 20.00 Tg compared to 2020, with grassland being the type with the largest change in overall carbon storage under the scenario, with a projected decrease of 94.54 Tg, an increase of 4.43 Tg in carbon storage in built-up, and an increase of 65.24 Tg in carbon storage in forests. In the urban development scenario, total carbon storage decreases by 54.65 Tg, mainly attributable to lower grassland area, which reduces carbon storage in the grassland area by

98.42 Tg, and extensive land is transformed to built-up, this would result in an increase of 9.60 Tg of carbon storage on building sites. In the context of ecological protection scenario, the total carbon storage is projected to increase by 197.55 Tg, comprising significant gains. Specifically, the carbon storage of forest is anticipated to rise by 370.12 Tg, and grassland by 544.26 Tg. Conversely, farmland carbon storage is expected to decrease by 177.93 Tg, while that of unutilised land is projected to decline by 51.91 Tg. Despite maintaining a trend of expansion, the rate of growth in built-up land has slowed down, contributing an additional 3.01 Tg to carbon storage over a decade. The farmland protection scenario is anticipated to result in the most significant reduction in carbon stocks, with total carbon storage reduced by 220.39 Tg. This primary loss is attributable to greenfield, with the carbon of grassland projected to decline by 188.92 Tg and forest anticipated to reduce by 255.45 Tg.

Table 4. Estimated and projected carbon storage (Tg) of different land type and total carbon storage in the Sichuan–Chongqing region (A, B, C, and D represent the scenarios of natural development, urban development, ecological protection, and farmland protection).

Land Type	Year			Scenario			
	2010	2015	2020	A	B	C	D
Farmland	1904.27	1896.67	1886.17	1901.22	1888.54	1708.24	2126.13
Forest	5337.45	5331.35	5495.49	5560.73	5540.70	5865.61	5240.04
Grassland	3528.75	3525.04	3366.77	3272.23	3268.35	3421.03	3177.85
Water	21.22	22.56	25.88	25.88	25.88	25.88	25.88
Built-up	11.23	15.30	20.74	25.17	30.34	23.75	21.41
Unused	327.15	309.97	310.84	300.65	297.43	258.93	294.18
Total	11,130.07	11,100.89	11,105.88	11,085.88	11,051.23	11,303.43	10,885.49

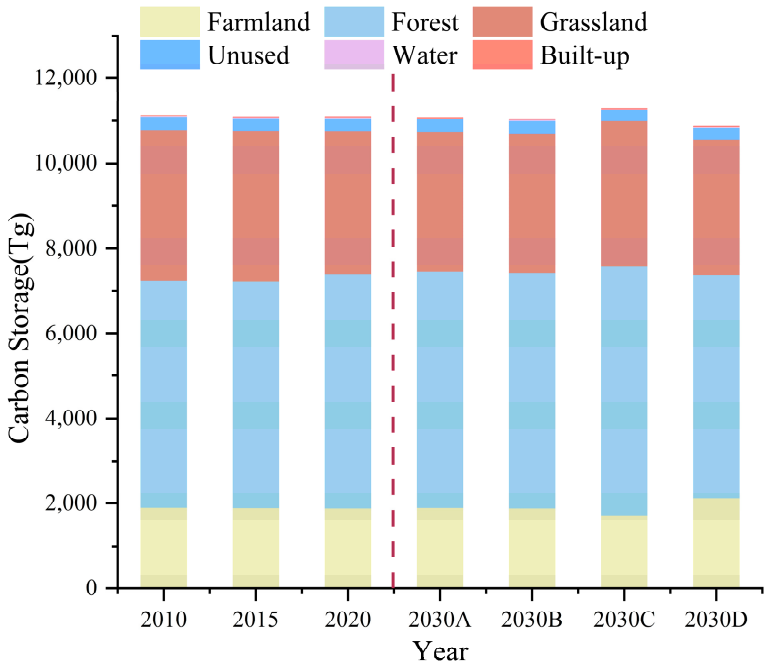


Figure 5. Estimated and projected carbon stocks from 2010 to 2030 (the left side of the red dotted line represents estimated carbon stocks from 2010 to 2020, while the right side displays projected carbon stock values in 2030 under various scenarios. A, B, C, and D represent the scenarios of natural development, urban development, ecological protection, and farmland protection in the Sichuan–Chongqing region in 2030, respectively).

3.3. The Drivers of Land Types and Carbon Storage Dynamics in the Sichuan–Chongqing Area

For clarification of the causes of land change in the Sichuan–Chongqing region, the LEAS module was applied to find the primary drivers of dynamic changes in each land type. The parameterisation of the LEAS module were detailed in Table A4. As illustrated in Figure 6, there are notable differences in the primary drivers of land type and carbon storage dynamics. For farmland, the primary driver was slope, with a contribution rate of 0.203, while economic factors such as GDP also had a substantial influence, contributing 0.147. Forests were primarily driven by slope (0.124) and DEM (0.098). Grassland dynamics were more closely tied to the climatic conditions of the Sichuan–Chongqing region, with temperature contributing 0.164. The drivers of built-up land dynamics differed significantly from those of farmland, forest, and grassland, as the most significant influences were no longer natural factors like slope and temperature, but rather economic factors such as GDP and population, contributing 0.264 and 0.248 respectively, far exceeding the contributions of other drivers. The drivers of unused land were diverse, with both natural factors like DEM and temperature and anthropogenic factors such as population size playing significant roles.

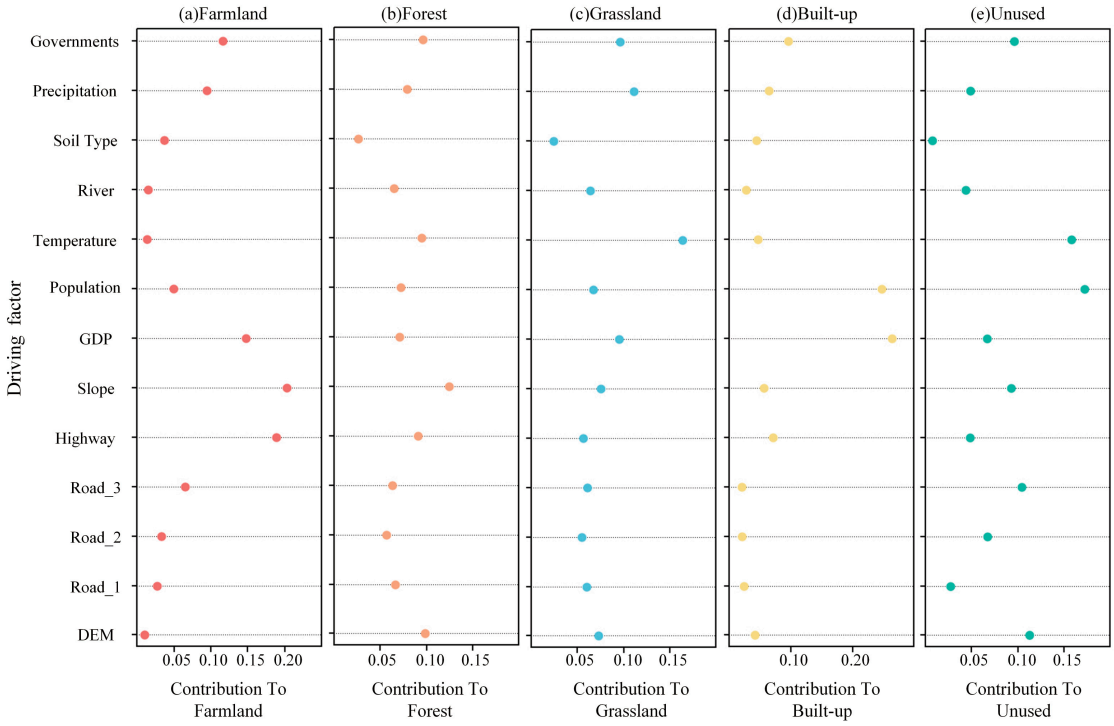


Figure 6. Contribution of land use and carbon storage change drivers to individual land types in the Sichuan–Chongqing region.

4. Discussion

4.1. Impacts of Natural Conditions and Anthropogenic Activities upon the Dynamics of Land Types

The distribution of land use in the Sichuan–Chongqing region is characterised by a high degree of complexity. Farmland, forest and grassland are found in patterns that are adapted to the natural conditions of the region. The Sichuan–Chongqing area is distinguished by strong topographical differences, an uneven temporal and spatial distribution of precipitation and significant regional heterogeneity [35]. In the western and southern regions of Sichuan, mountain plains and valleys alternating, and owing to the complex topography, higher average altitude and lower average annual temperature, these conditions are not conducive to the development of farmland. This has resulted in a relatively slower pace of agricultural development and a cultivated land area that is smaller than that of the eastern region. On the other hand, the Sichuan Basin in the eastern part of the

Sichuan–Chongqing region lies on a flat terrain and is abundant in water resources, providing unique natural conditions for farmland development, and the interactions and changes in these natural factors affect farmers' decisions concerning farmland use. In addition, the dynamics of forests and grasslands are closely related to natural factors. Western Sichuan has 60% of the forest resources and more than 90% of the grasslands in Sichuan Province, with forests consisting mainly of alpine coniferous forests with high resistance to cold and grasslands consisting mainly of thickets and grasslands. The spatial heterogeneity of these natural conditions has important implications for differences in the spatial distribution of carbon density [36].

In addition to natural conditions, human activities also have a major impact on land use dynamics, especially built-up land in the Sichuan–Chongqing region, where the driving force for built-up land is mainly population and GDP. Regions with large populations tend to generate new built-up land, and population growth drives urban development and expansion [37], which causes cities to continue to extend outwards, occupying increasingly undeveloped land. On the other hand, the area of Sichuan is unbalanced in its development, with economic and social development more rapid than agricultural development [38], and urban economic development requires more land to improve infrastructure such as housing, factories and commercial facilities. As industrialisation and urbanisation progress, some forests and grasslands may be used for built-up infrastructure. It is thus imperative to develop and utilise finite resources in a rational manner, formulate scientific planning and management measures, and give due consideration to factors such as topography, natural conditions and the ecological environment in order to achieve sustainable development.

4.2. The Impact of Urbanisation on the Change in Carbon Storage in the Sichuan–Chongqing Region

Over the past decade, there has been intense urban expansion in the Sichuan–Chongqing region [39], resulting in an increasing demand for construction and industrial land and a decreasing area of collective rural land and farmland. Specifically, in the context of urbanisation, activities such as the logging of forests and the reclamation of wasteland have been observed, and the expansion of land development has become increasingly frequent, causing severe damage to the ecosystem. Areas of land with high carbon density, such as forests and grasslands, has been decreasing, while the size of built-up land with relatively low carbon density has been increasing dramatically, which has led to a decrease in the overall carbon sequestration capacity in the Sichuan–Chongqing region. Furthermore, excessive grazing and exploitation have also harmed grasslands and soils, leading to a decline in soil quality and a reduction in plant cover, which has significantly affected the ability to store and fix carbon. Between 2015 and 2020, the total carbon storage in this region slightly rebounded. This suggests that the region has accelerated its ecological development and environmental protection efforts in recent years. Effective measures, such as scientific planting, regular cleaning, and fire prevention, have been taken to improve the ecological level during the urbanisation process. Policies promoting forest growth and protection have increased carbon storage. The "double carbon" policy has also facilitated the conversion of farmland to more carbon-intensive forests and grasslands, resulting in significant progress.

4.3. Differences in Land Types and Carbon Storage Under the Complex Terrain of the Sichuan–Chongqing Region

The diverse and intricate terrain units in the Sichuan–Chongqing region, including mountains, plateaus, hills, basins, and plains, result in rugged and uneven land surfaces, as well as heterogeneous vegetation distributions [40]. Topographic factors such as slope and DEM play key roles in land distribution patterns and carbon storage distributions in complex terrain areas. In this study, the degree of surface undulation was calculated from DEM data, and the landforms of the Sichuan–Chongqing region were classified into six categories on the basis of the degree of surface undulation: plains, plateaus, hills, low-relief mountains, middle-relief mountains, and high-relief mountains [41]. As shown in Figures 7 and 8, farmland and built-up land are concentrated in relatively flat plains and

tableland areas that exhibit low carbon storage, such as Chengdu, Chongqing Municipality and the surrounding areas. In contrast, the land types in medium and high rolling hills are dominated by those with higher carbon storage per unit area, such as forests and grasslands. Examples of these landscapes include the western Sichuan plateau region. Overall, the distributions of land use and carbon storage in the Sichuan–Chongqing region are closely related to topographic relief. Carbon storage is lower in flat areas and higher in steep mountainous areas. This study's results provide an essential reference for land resource management and carbon storage assessment in the region. This study also offers a new perspective on the influence of complex topography on the carbon cycle. In the future, further investigations can be conducted on the interactions between topographic factors and other factors, such as vegetation type and soil properties, to comprehensively explore the mechanism of topographic influences on carbon storage distribution.

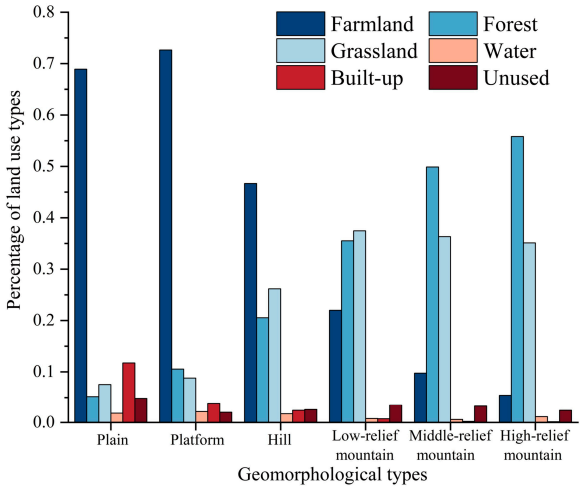


Figure 7. Land use distribution in the Sichuan–Chongqing region under various landforms.

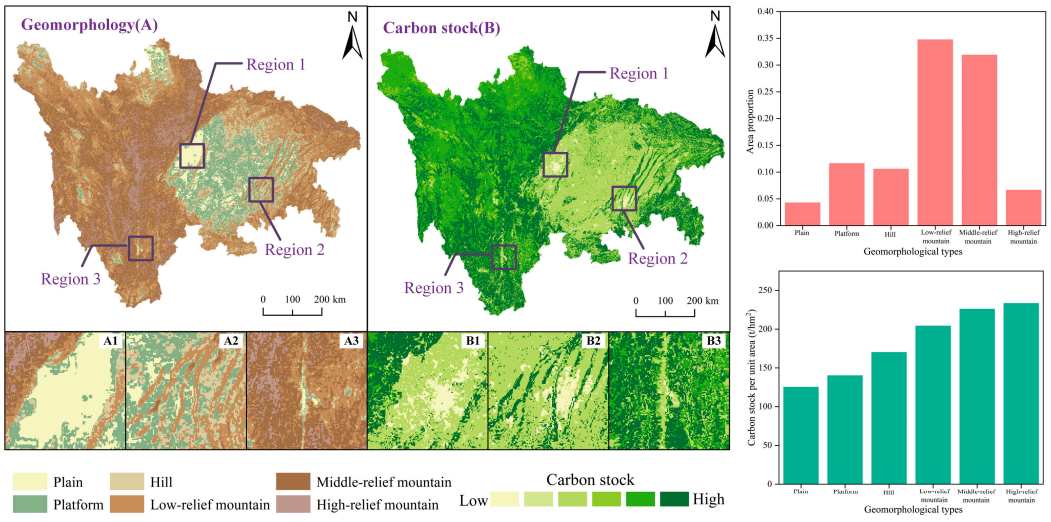


Figure 8. Carbon stock distribution and geomorphological distribution in the Sichuan–Chongqing region ((**A**,**B**) represent the geomorphological distribution and carbon stock distribution in the Sichuan–Chongqing region, respectively; Regions 1, 2 and 3 are enlarged example regions; and the statistical graphs on the right side represent the proportion of geomorphological landforms and the average carbon stock of geomorphological landforms, respectively).

4.4. The Uncertainty of the Research Study

In this study, the InVEST model was employed to calculate the carbon density of land types per unit area in the Sichuan–Chongqing region as a basis for carbon storage

estimation. Given the disparate sources of carbon density data and references, as well as the discrepancies in the natural conditions of the specific study area and the human activity conditions, there are some discrepancies between the estimated regional carbon storage in this study and that of some previous relevant studies [42,43]. The InVEST model, however, is a simplified carbon density estimation model that divides the carbon pools into four categories and assumes that the carbon density per unit area of each land type remains constant. Nevertheless, it is important to note that carbon storage may change over time due to a number of factors, including natural conditions, human activities or other factors. In this study, to account for the differences in climatic conditions between the Sichuan–Chongqing region and other regions, precipitation was introduced to correct the InVEST model, with the aim of ensuring that the carbon storage estimation results are as close to the real values as possible. However, it should be noted that the final results inevitably contain some degree of error.

To explore the main drivers of land use change and carbon storage change in the Sichuan–Chongqing region, the PLUS model was used to select natural drivers and socioeconomic factors, such as DEM, slope, GDP, and population, that could be used to assess the drivers of change in land accurately and further analyse the drivers of carbon storage [44–46]. Moreover, the CA module was also used to model future land use under different policy priorities, with a kappa coefficient of 0.892 and a FOM value of 0.191 for simulating the 2020 results against the 2010 land use results prior to the formal simulation. However, although such accuracy indicates that the PLUS model has high precision and reliability and can be used to predict the future distribution of land use in the Sichuan–Chongqing region, when it is applied to project future land use scenarios, deviations from actual trends may occur and could be exacerbated by the lack of relevant data post-2020 for more precise estimations.

In light of the above, future research should more fully consider the conditions of natural and anthropogenic factors, utilise more accurate data to estimate carbon storage in combination with field surveys, and consider the spatial inhibition of land types and the age structure of vegetation among other factors which have an impact on carbon density. Furthermore, a greater number of factors should be considered during the process of multi-scenario modelling, and more flexible and accurate scenario rules should be formulated in conjunction with different policies with the aim of obtaining more accurate land use modelling results and calculating carbon storage with greater precision.

5. Conclusions

This study focuses on the Sichuan–Chongqing region. Land use data and carbon density data were used to calculate the carbon storage per unit area for each land type according to the InVEST model. The model was refined via annual precipitation data. The analysis of changes in carbon storage linked to land use transformations and the driving forces behind such changes from 2010 to 2020 was enabled by employing the PLUS model alongside DEM, GDP, population, and other relevant data. Additionally, the study examined differences in the distributions of land types across diverse landforms within the intricate topography of the Sichuan–Chongqing region and their associated carbon storage implications. A multi-scenario simulation for the land use projection in 2030 was conducted to assess carbon storage under various scenarios and explore temporal and spatial shifts in carbon storage trends. The following conclusions were obtained:

(1) The land types in the Sichuan–Chongqing region are concentrated, with forests being the dominant type. The proportion of built-up land exceeds China's average farmland share (14.3%) but is below the national average for built-up land (4%). Built-up land exhibited the most significant temporal fluctuations—increasing from 0.83% in 2010 to 1.52% in 2020—whereas areas of grassland, farmland, and unused land decreased.

(2) The total carbon storage for each land type was calculated using the modified InVEST model. Forestland had the highest carbon storage per unit area at 275.86 t/hm^2. From 2010 to 2020, the Sichuan–Chongqing region experienced a decline in total carbon storage

from 111,130.07 Tg to 11,105.88 Tg, indicating a reduction of 24.19 Tg. The PLUS model demonstrated a kappa value of 0.892 and an FOM value of 0.191. These results suggest that the PLUS model is appropriate for simulating the expected land use distribution in the Sichuan–Chongqing region. The results of our multi-scenario prediction show that except for the ecological development scenario, the total carbon storage in different development scenarios will decline. The farmland protection scenario shows the most significant decline in total carbon storage, with a projected reduction of 220.39 Tg.

(3) The decline in carbon storage is attributed primarily to the encroachment of urban development into agricultural land, forests, and grasslands, leading to a reduction in high-carbon-density regions and an increase in low-carbon-density areas. Natural factors, including slope and temperature, significantly influence agricultural land, forests, and grasslands, whereas economic factors such as GDP and population growth are driving forces behind the continuous expansion of urbanised areas. Moreover, the distribution of land use and carbon storage in the Sichuan–Chongqing region is intricately linked to its diverse topography, where flat regions present lower carbon storage levels and steep mountainous areas present higher carbon storage capacities.

Author Contributions: Conceptualization, Tiankuo Chu and Xiaoai Dai; methodology, Tiankuo Chu; validation, Tiankuo Chu, Jun Li, and Chengye Zhang; formal analysis, Tiankuo Chu; investigation, Tiankuo Chu; resources, Tiankuo Chu; data curation, Tiankuo Chu; writing—original draft preparation, Tiankuo Chu, Huan Huang, and Manling Peng; writing—review and editing, Jun Li, Chengye Zhang, Xiaoai Dai, and Yikun Qing; supervision, Xiaoai Dai; funding acquisition, Jun Li and Chengye Zhang All authors have read and agreed to the published version of the manuscript.

Funding: This work was founded by the National Natural Science Foundation of China Grant (42271480, 42371347) and The Science and Technology Development Plan Project of the Silk Road Economic Belt Innovation-Driven Development Pilot Zone and the Urumqi-Changji-Shihezi National Innovation Demonstration Zone Grant (2023LQY02).

Institutional Review Board Statement: Not applicable.

Informed Consent Statement: Not applicable.

Data Availability Statement: Data are contained within the article.

Conflicts of Interest: The authors declare no conflicts of interest.

Appendix A

Table A1. Carbon density of each land use in Sichuan–Chongqing region (t/hm^2).

Land Type	Above-Ground Carbon Storage	Underground Carbon Storage	Soil Carbon Storage
Farmland	23.48	1.33	97.37
Forest	142.77	10.53	122.56
Grassland	69.18	26.78	98.24
Water	1.45	0.00	42.47
Built-up	0.00	0.00	24.10
Unused	8.62	0.00	170.51

Table A2. Land use transfer matrix for the Sichuan–Chongqing region, 2010–2020 (million hm^2).

Land Type	2020								
		Grassland	Farmland	Built-up	Forest	Water	Unused	Total	Transfer out
2010	Grassland	1229.13	115.13	4.39	385.23	9.56	73.63	1817.07	587.94
	Farmland	95.87	1092.01	49.17	298.51	22.59	0.43	1558.58	466.57
	Built-up	1.5	18.08	21.38	3.71	1.9	0.04	46.61	25.23
	Forest	330.98	295.81	7.47	1285.43	7.86	7.29	1934.84	649.41

Table A2. *Cont.*

Land Type	2020							
		Grassland	**Farmland**	**Built-up**	**Forest**	**Water**	**Unused**	**Total**	**Transfer out**
	Water	5.13	18.81	3.51	4.34	15.45	1.07	48.31	32.86
	Unused	71.05	3.92	0.12	14.91	1.56	91.06	182.62	91.56
	Total	1733.66	1543.76	86.04	1992.13	58.92	173.52	5588.03	1853.57
	Transfer to	504.53	451.75	64.66	706.7	43.47	82.46	1853.57	

Table A3. CA module parameter setting.

Parameters	**Neighbourhood Size: 5**	**Patch Generate: 0.5**	**Expansion Coefficient: 0.1**	**Percentage of Seeds: 0.0001**
Domain weight	Farmland 0.196	Forest 0.130	Grassland 0.427	Built-up 0.140	Unused 0.073

Table A4. LEAS module parameter setting.

Parameters	**Sampling Rate**	**Number of Regression Tree**	**Sample Module**	**mTry**	**Thread**
	0.02	20	Random sampling	13	4

References

1. Tian, H.; Melillo, J.; Lu, C.; Kicklighter, D.; Liu, M.; Ren, W.; Xu, X.; Chen, G.; Zhang, C.; Pan, S.; et al. China's terrestrial carbon balance: Contributions from multiple global change factors. *Glob. Biogeochem. Cycles* **2011**, *25*, GB1007. [CrossRef]
2. Yang, H.; Huang, J.; Liu, D. Linking climate change and socioeconomic development to urban land use simulation: Analysis of their concurrent effects on carbon storage. *Appl. Geogr.* **2020**, *115*, 102135. [CrossRef]
3. Midgley, G.F.; Bond, W.J.; Kapos, V.; Ravilious, C.; Scharlemann, J.P.W.; Woodward, F.I. Terrestrial carbon stocks and biodiversity: Key knowledge gaps and some policy implications. *Curr. Opin. Environ. Sustain.* **2010**, *2*, 264–270. [CrossRef]
4. Quay, P.D.; Tilbrook, B.; Wong, C.S. Oceanic Uptake of Fossil Fuel CO_2: Carbon-13 Evidence. *Science* **1992**, *256*, 74–79. [CrossRef]
5. Abu-Hashim, M.; Elsayed, M.; Belal, A.-E. Effect of land-use changes and site variables on surface soil organic carbon pool at Mediterranean Region. *J. Afr. Earth Sci.* **2016**, *114*, 78–84. [CrossRef]
6. Houghton, R.; Goodale, C. Effects of land-use change on the carbon balance of terrestrial ecosystems. *Ecosyst. Land Use Change* **2004**, *9*, 85–98. [CrossRef]
7. Fang, J.; Chen, A.; Peng, C.; Zhao, S.; Ci, L. Changes in forest biomass carbon storage in China between 1949 and 1998. *Science* **2001**, *292*, 2320–2322. [CrossRef]
8. Guo, J.; Zhang, R.P.; Wang, R.H.; Yusupujiang, A.; Asiyemu, T.; Zhang, D.Y. Estimation of carbon storage and carbon density of forest vegetation in Ili River Valley, Xinjiang. In Proceedings of the IOP Conference Series: Earth and Environmental Science, Beijing, China, 7–8 July 2016; pp. 12–27. [CrossRef]
9. Jung, M.; Reichstein, M.; Margolis, H.A.; Cescatti, A.; Richardson, A.D.; Arain, M.A.; Arneth, A.; Bernhofer, C.; Bonal, D.; Chen, J.Q.; et al. Global patterns of land-atmosphere fluxes of carbon dioxide, latent heat, and sensible heat derived from eddy covariance, satellite, and meteorological observations. *J. Geophys. Res. Biogeosci.* **2011**, *116*, G00J07. [CrossRef]
10. Pan, Y.D.; Birdsey, R.A.; Fang, J.Y.; Houghton, R.; Kauppi, P.E.; Kurz, W.A.; Phillips, O.L.; Shvidenko, A.; Lewis, S.L.; Canadell, J.G.; et al. A Large and Persistent Carbon Sink in the World's Forests. *Science* **2011**, *333*, 988–993. [CrossRef]
11. Piao, S.; He, Y.; Wang, X.; Chen, F. Estimation of China's terrestrial ecosystem carbon sink: Methods, progress and prospects. *Sci. China Earth Sci.* **2022**, *65*, 641–651. [CrossRef]
12. Sun, B.Q.; Du, J.Q.; Chong, F.F.; Li, L.J.; Zhu, X.Q.; Zhai, G.Q.; Song, Z.B.; Mao, J.L. Spatio-Temporal Variation and Prediction of Carbon Storage in Terrestrial Ecosystems in the Yellow River Basin. *Remote Sens.* **2023**, *15*, 3866. [CrossRef]
13. Melillo, J.M.; McGuire, A.D.; Kicklighter, D.W.; Moore, B.; Vorosmarty, C.J.; Schloss, A.L. Global climate-change and terrestrial net primary production. *Nature* **1993**, *363*, 234–240. [CrossRef]
14. Sun, Q.L.; Li, B.L.; Zhang, T.; Yuan, Y.C.; Gao, X.Z.; Ge, J.S.; Li, F.; Zhang, Z.J. An improved Biome-BGC model for estimating net primary productivity of alpine meadow on the Qinghai-Tibet Plateau. *Ecol. Model.* **2017**, *350*, 55–68. [CrossRef]
15. Potter, C.S.; Randerson, J.T.; Field, C.B.; Matson, P.A.; Vitousek, P.M.; Mooney, H.A.; Klooster, S.A. Terrestrial ecosystem production—A process model-based on global satellite and surface data. *Glob. Biogeochem. Cycles* **1993**, *7*, 811–841. [CrossRef]

16. Zhang, C.; Li, F.; Li, J.; Xing, J.; Yang, J.; Guo, J.; Du, S. Recognition of land use on open-pit coal mining area based on DeepLab v3+ and GF-2 high-resolution images. *Coal Geol. Explor.* **2022**, *50*, 94–103. [CrossRef]
17. Yan, M.; Li, Z.Y.; Tian, X.; Chen, E.X.; Zhang, W.F.; Guo, Y.; Li, C.M. Simulation of carbon flux of forest ecosystem by Biome-BGC and MODIS-PSN models. In Proceedings of the IEEE Geoscience and Remote Sensing Symposium, Quebec City, QC, Canada, 13–18 July 2014; pp. 1065–1068. [CrossRef]
18. Guo, L.B.; Gifford, R.M. Soil carbon stocks and land use change: A meta analysis. *Glob. Change Biol.* **2022**, *8*, 345–360. [CrossRef]
19. Zhao, Z.; Liu, G.; Mou, N.; Xie, Y.; Xu, Z.; Li, Y. Assessment of carbon storage and its influencing factors in Qinghai-Tibet Plateau. *Sustainability* **2018**, *10*, 1864. [CrossRef]
20. Zhao, M.; He, Z.; Du, J.; Chen, L.; Lin, P.; Fang, S. Assessing the effects of ecological engineering on carbon storage by linking the CA-Markov and InVEST models. *Ecol. Indic.* **2019**, *98*, 29–38. [CrossRef]
21. Babbar, D.; Areendran, G.; Sahana, M.; Sarma, K.; Raj, K.; Sivadas, A. Assessment and prediction of carbon sequestration using Markov chain and InVEST model in Sariska Tiger Reserve, India. *J. Clean Prod.* **2021**, *278*, 123333. [CrossRef]
22. Krcmar, E.; Stennes, B.; van Kooten, G.C.; Vertinsky, I. Carbon sequestration and land management under uncertainty. *Eur. J. Oper. Res.* **2001**, *135*, 616–629. [CrossRef]
23. Chen, Y.; Cui, J.; He, L.; Men, M. Optimal Simulation of the Land-Use Structure Based on the Local Ecological Environment: The Case of Huanghua City in Hebei Province, China. *Rev. Bras. Cienc. Solo* **2019**, *43*, e0180063. [CrossRef]
24. Liu, X.; Liang, X.; Li, X.; Xu, X.; Ou, J.; Chen, Y.; Li, S.; Wang, S.; Pei, F. A future land use simulation model (FLUS) for simulating multiple land use scenarios by coupling human and natural effects. *Landsc. Urban Plan.* **2017**, *168*, 94–116. [CrossRef]
25. Liang, X.; Guan, Q.; Clarke, K.C.; Liu, S.; Wang, B.; Yao, Y. Understanding the drivers of sustainable land expansion using a patch-generating land use simulation (PLUS) model: A case study in Wuhan, China. *Comput. Environ. Urban Syst.* **2021**, *85*, 101569. [CrossRef]
26. Sharp, R.; Tallis, H.; Ricketts, T.; Guerry, A.; Wood, S.; Chaplin-Kramer, R.; Nelson, E.; Ennaanay, D.; Wolny, S.; Olwero, N. *InVEST 3.10 User's Guide*; Collaborative Publication by the Natural Capital Project; Stanford University: Stanford, CA, USA; The University of Minnesota: Minneapolis, MN, USA; The Nature Conservancyy: Arlington, VA, USA; World Wildlife Fund: Morges, Switzerland, 2018.
27. Zhou, J.J.; Zhao, Y.R.; Huang, P.; Zhao, X.; Feng, W.; Li, Q.Q.; Xue, D.X.; Dou, J.; Shi, W.; Wei, W.; et al. Impacts of ecological restoration projects on the ecosystem carbon storage of inland river basin in arid area, China. *Ecol. Indic.* **2020**, *118*, 106803. [CrossRef]
28. Xu, L.; He, N.; Yu, G. A dataset of carbon density in Chinese terrestrial ecosystems (2010s). *China Sci. Data* **2019**, *4*, 90–96. [CrossRef]
29. Fang, J.-Y.; Wang, Z.M. Forest biomass estimation at regional and global levels, with special reference to China's forest biomass. *Ecol. Res.* **2001**, *16*, 587–592. [CrossRef]
30. Huang, M.; Ji, J.; Cao, M.; Li, K. Modeling study of vegetation shoot and root biomass in China. *Acta Ecol. Sin.* **2006**, *26*, 4156–4163. [CrossRef]
31. Alam, S.A.; Starr, M.; Clark, B.J. Tree biomass and soil organic carbon densities across the Sudanese woodland savannah: A regional carbon sequestration study. *J. Arid. Environ.* **2013**, *89*, 67–76. [CrossRef]
32. Gao, L.; Tao, F.; Liu, R.; Wang, Z.; Leng, H.; Zhou, T. Multi-scenario simulation and ecological risk analysis of land use based on the PLUS model: A case study of Nanjing. *Sustain. Cities Soc.* **2022**, *85*, 104055. [CrossRef]
33. Lou, Y.; Yang, D.; Zhang, P.; Zhang, Y.; Song, M.; Huang, Y.; Jing, W. Multi-Scenario Simulation of Land Use Changes with Ecosystem Service Value in the Yellow River Basin. *Land* **2022**, *11*, 992. [CrossRef]
34. Wu, Y.Z.; Zhang, X.L.; Shen, L.Y. The impact of urbanization policy on land use change: A scenario analysis. *Cities* **2011**, *28*, 147–159. [CrossRef]
35. Ji, T.; Li, G.; Yang, H.; Liu, R.; He, T. Comprehensive drought index as an indicator for use in drought monitoring integrating multi-source remote sensing data: A case study covering the Sichuan-Chongqing region. *Int. J. Remote Sens.* **2018**, *39*, 786–809. [CrossRef]
36. Gao, X.; Gray, J.; Cohrs, C.W.; Cook, R.; Albaugh, T.J. Longer greenup periods associated with greater wood volume growth in managed pine stands. *Agric. For. Meteorol.* **2021**, *297*, 108237. [CrossRef]
37. Zou, D.; Cong, H. Data driven based coordinated development pattern and influencing factor analysis using spatial and temporal data. *Clust. Comput.* **2019**, *22*, S9991–S10007. [CrossRef]
38. Xiao, M.; Zhang, Q.; Qu, L.; Hussain, H.A.; Dong, Y.; Zheng, L. Spatiotemporal Changes and the Driving Forces of Sloping Farmland Areas in the Sichuan Region. *Sustainability* **2019**, *11*, 906. [CrossRef]
39. Song, Y.; Jiao, L.; Liu, J.; Xu, G. Analysis of the factors affecting the degree of urban expansion: Taking Wuhan city as an example. *Geomat. Inf. Sci. Wuhan Univ.* **2021**, *46*, 417–426. [CrossRef]
40. Shao, J.A.; Li, Y.; Ni, J. The characteristics of temperature variability with terrain, latitude and longitude in Sichuan-Chongqing Region. *J. Geogr. Sci.* **2012**, *22*, 223–244. [CrossRef]
41. Cheng, W.; Zhou, C.; Chai, H.; Zhao, S.; Liu, H.; Zhou, Z. Research and compilation of the Geomorphologic Atlas of the People's Republic of China (1:1,000,000). *J. Geogr. Sci.* **2011**, *21*, 89–100. [CrossRef]
42. Wu, D.; Zhu, K.; Zhang, S.; Huang, C.; Li, J. Evolution Analysis of Carbon Storage in Chengdu-Chongqing Economic Zone Based on PLUS Model and InVEST Model. *Ecol. Environ. Monit. Three Gorges* **2022**, *7*, 1–18. [CrossRef]

43. Xiang, M.; Wang, C.; Tan, Y.; Yang, J.; Duan, L.; Fang, Y.; Li, W.; Shu, Y.; Liu, M. Spatio-temporal evolution and driving factors of carbon storage in the Western Sichuan Plateau. *Sci. Rep.* **2022**, *12*, 8114. [CrossRef]
44. Li, P.; Chen, J.; Li, Y.; Wu, W. Using the InVEST-PLUS Model to Predict and Analyze the Pattern of Ecosystem Carbon storage in Liaoning Province, China. *Remote Sens.* **2023**, *15*, 4050. [CrossRef]
45. Wang, Z.; Zeng, J.; Chen, W. Impact of urban expansion on carbon storage under multi-scenario simulations in Wuhan, China. *Environ. Sci. Pollut. Res.* **2022**, *29*, 45507–45526. [CrossRef] [PubMed]
46. Zhu, L.; Song, R.; Sun, S.; Li, Y.; Hu, K. Land use/land cover change and its impact on ecosystem carbon storage in coastal areas of China from 1980 to 2050. *Ecol. Indic.* **2022**, *142*, 109178. [CrossRef]

Disclaimer/Publisher's Note: The statements, opinions and data contained in all publications are solely those of the individual author(s) and contributor(s) and not of MDPI and/or the editor(s). MDPI and/or the editor(s) disclaim responsibility for any injury to people or property resulting from any ideas, methods, instructions or products referred to in the content.